



Published in final edited form as:

Health Phys. 2012 October ; 103(4): 400–410.

Evidence of Delayed Gastrointestinal Syndrome in High-Dose Irradiated Mice

Catherine Booth^{*}, Gregory Tudor^{*}, Nicola Tonge^{*}, Terez Shea-Donohue[†], and Thomas MacVittie^{††}

^{*}Epistem Ltd, Manchester, UK

[†]University of Maryland, Mucosal Biology Research Center, Baltimore, MD, USA

^{††}University of Maryland, School of Medicine, Dept. of Radiation Oncology, Baltimore, MD, USA

Abstract

The acute effects of irradiation on the gastrointestinal (GI) system are well documented but the longer-term effects are less well known. Increased incidence of adenocarcinoma has been noted but apart from descriptions of fibrosis, the development of other pathologies specific to survivors of acute radiation is poorly understood. Samples were taken from C57BL/6 mice irradiated with partial-body irradiation where the thorax, head and forelimbs were shielded (i.e. sparing 40% of the bone marrow). Tissue from age matched controls was also collected. There were clear pathological changes in the intestine associated with DEARE (Delayed Effects of Acute Radiation Exposure) at doses greater than 12 Gy, with a dose related increase in observed pathologies. Mice maintained on the synthetic antibiotic ciprofloxacin during the acute phase (days four to twenty), however, had a lower or delayed incidence of symptoms. After twenty days mice developed structures similar to early adenomas. Abnormally high levels of apoptotic and mitotic cells were present in some crypts, along with the early adenomas, suggesting tissue regeneration and areas of deregulated cell turnover. Over time, in animals with advanced symptoms there was inhibited crypt cell proliferation, a blunting of the crypts and villi and an enlargement of villus girth, with an increasingly acellular and fibrotic extracellular matrix (a characteristic that has been previously demonstrated in aging mice). Together these changes may lead to a reduced functional surface area and less motile intestine. These observations are similar to those seen in geriatric animals, suggesting a premature aging of the GI tract.

Keywords

radiation damage; radiation dose; mice; X rays; acute radiation exposure; gastrointestinal

INTRODUCTION

Radiation damage to the intestine, and consequential symptoms, are classified as acute or delayed (GI-ARS, gastrointestinal acute radiation syndrome; GI-DEARE, gastrointestinal delayed effects of acute radiation exposure). The acute phase occurs within days of exposure

Corresponding author: C Booth, Epistem Ltd, Manchester, UK, M13 9XX. Tel: +44 (0)161 606 7346, Fax: +44 (0)161 606 7348, c.booth@epistem.co.uk.

¹**Publisher's Disclaimer:** This is a PDF file of an unedited manuscript that has been accepted for publication. As a service to our customers we are providing this early version of the manuscript. The manuscript will undergo copyediting, typesetting, and review of the resulting proof before it is published in its final citable form. Please note that during the production process errors may be discovered which could affect the content, and all legal disclaimers that apply to the journal pertain.

and results from the loss of intestinal clonogenic cells, leading to loss of the epithelial crypts and ulceration. The severity of the mucosal barrier breakdown and ability of the tissue to repair the damage is radiation dose dependent, with GI-ARS being induced by doses higher than those that are lethal to the bone marrow. Thus, even if effective mitigation improves the intestinal epithelial regeneration process and increases animal survival through the GI-ARS timeframe, one will inevitably succumb to hematological acute radiation syndrome (H-ARS) shortly afterwards. However, in reality it is likely that a small fraction of the bone marrow will survive a radiation incident, which may be sufficient to repopulate the hematopoietic system and allow long term survival. In such cases the long term effects on the intestine, which are largely uncharacterized, will need to be understood and treated.

Evidence that the delayed effects of radiation exposure are likely to be a problem comes not only from the Japanese survivors of such exposure, but also from radiation oncology. For example, patients receiving local radiation exposure to the abdomen and pelvis (and hence minimal overall bone marrow involvement) frequently develop both acute and delayed intestinal enteropathies (Dubois and Walker 1988, Johnson and Carrington 1992, Hauer-Jensen 1990, Kao 1995). The latter tends to occur months to years post irradiation (where the rapid cell turnover will have already replaced the intestinal surface epithelium tens to hundreds of times). The pathology of this delayed response is characterized by intestinal fibrosis and vascular sclerosis leading to a variety of complications that require surgery within five years in 5% of cases (Coia et al. 1995). However, there is a much greater incidence of sustained gastrointestinal symptoms (from diarrhea and constipation to obstruction, fistulation and sepsis), estimated to occur in half of patients receiving irradiation for the treatment of pelvic tumors (prostate, gynecological, and anorectal) (Hauer-Jensen 2003, Andreyev 2005). Details of the incidence of intestinal tumorigenesis as a result of such clinical exposure is more difficult to define (due to the disparate nature of the patient treatments, ages, presentation of symptoms and diagnosis relative to other diseases and treatments and overall demographic), but it is clear from survivors of nuclear incidents that over the long term there is also an increased risk of GI tumors following radiation exposure (Goodman et al. 1994; Thompson et al. 1994).

In order to therefore develop medical countermeasures to treat the prolonged or delayed GI damage it is necessary to first understand the pathology and its causes. Crucial is the characterization of the timelines of the development of DEARE in relation to radiation dose. Langberg et al. (1996) measured the radiation dose response of exteriorized loops of rat small bowel that were relocated and locally irradiated in the scrotum. Fibrosis, measured by collagen assay and radiation injury score, increased with total dose. Whilst informative of the expected pathologies, this model did not represent the extent of radiation exposure that may be experienced following more widespread exposure. Hauer-Jensen (1990) reviewed the general pathologies of late radiation injury in the small intestine that were experienced both in the laboratory and oncology clinic. Intestinal wall fibrosis and vascular sclerosis were highlighted as major areas of concern.

We have therefore allowed a number of animals that survived highly controlled GI-ARS following a range of radiation doses from 8 Gy to 16 Gy (Booth et al. this issue) to age for up to a further six months tracing the development of both symptoms and histopathologies. Crucially, these data were then compared with histopathology from age matched control mice in order to distinguish the results from those of simple gut aging.

MATERIALS AND METHODS

All procedures were certified according to the UK Animal (Scientific Procedures) Act 1986. Male C57BL/6 mice aged eight to ten weeks were purchased from Harlan UK and allowed

to acclimatize for two weeks prior to irradiation. All mice were held in individually ventilated cages (IVCs) in a specific pathogen free (SPF) barrier unit. A twelve hour light:dark cycle was maintained with lights being turned on at approximately 0700 hours and off at approximately 1900 hours. There was a constant room temperature of $21 \pm 2^\circ\text{C}$ and a mean relative humidity of $55 \pm 10\%$. The animals received 2018 extruded rodent diet (Harlan UK) and sterile acidified water (ad libitum) from time of arrival and throughout the study. Animals were identified by ear punches in cages labeled with the appropriate information necessary to identify the study, dose, animal number and treatment groups.

Other supportive care was administered as indicated in the results. Ciprofloxacin (0.67g L^{-1}) was administered in the drinking water and was also used to wet the food and generate mash, supplied within the cage to allow for easier access by mice potentially weakened from radiation exposure. Acidified water was used to wet the food for those animals without supportive care. Observations by Orschell et al (this issue) have shown that the presence of Ciprofloxacin in the water does not alter the level of water consumption by the mice.

Animals were irradiated at 15:00 \pm one hour. Irradiation was performed using a Pantak HF320 X ray set (Agfa NDT Ltd, Reading, UK), operated at 300kV, 10mA. The X-ray tube has additional filtration to give a radiation quality of 2.3mm Copper half-value layer (HVL). Mice were restrained in a compartmentalized perspex jig, positioned at a distance of 700mm from the focus of the X-ray tube. Mice were irradiated in a field allowing irradiation of up to twelve mice simultaneously. Dosimetry was checked every two months during which time it has remained within $\pm 1\%$ of the original value. QA and control procedures were performed prior to and during each irradiation to confirm dose and energy output remain within range.

Animals received partial body irradiation and were anaesthetized with Ketamine (Fort Dodge) and Rompun (Bayer) administered intraperitoneally to allow immobilization and accurate lead shielding of the appropriate area. Animals had the head, forelimbs and thorax shielded (estimated to protect approximately 40% of the bone marrow, PBI BM40) (Boggs 1984). Irradiation was delivered at a dose rate of 70.0 cGy min^{-1} .

All animals were weighed and their well being inspected daily from the initiation of treatment to the end of the study. Any animal demonstrating more than 15% weight loss was considered unwell and humanely euthanized if the weight loss was sustained at greater than 20% for 24 hours and mice also demonstrated signs of a moribund state (withdrawn behavior, reduced body temperature as judged by feeling cool to touch, lack of grooming and dehydration as judged by a persistent skin tent on pinching). Mice with over 20% weight loss and developing moribund symptoms were euthanized. All other animals were euthanized at scheduled times (75 to 192 days). The mice were injected i.p. with 0.5ml of a 20mg/ml solution of Bromodeoxyuridine (BrdU) (Sigma B5002) forty minutes prior to euthanasia.

The small intestine and colon were removed, flushed and cut in two, with half fixed in Carnoy's fixative for 30 to 60 minutes and half fixed in formalin for 18 to 24 hours. They were then transferred to 70% ethanol prior to processing for histology to provide one paraffin embedded tissue block per mouse.

The intestines were 'bundled' prior to embedding in order to obtain the ideal orientation of the crypts (see Booth et al. in this issue). Each paraffin block generated was then sectioned ($3\mu\text{m}$ sections) to provide three slides per block, each slide containing two non serial sections. The slides were then stained for hematoxylin and eosin (H & E), BrdU and Masson Trichrome.

H & E staining protocol

Paraffin sections were dewaxed in xylene and rehydrated through a series of alcohols to water using a Leica Autostainer XL ST5010. Once they were rehydrated the slides were immersed in Gill's 2 Hematoxylin (ThermoFisher 6765007) for one minute, rinsed in running water for one minute, dipped in alkaline water then rinsed, before being immersed in Eosin (ThermoFisher 6766009) for one minute. Sections were then rinsed in water, dehydrated and cleared in xylene using the Leica Autostainer XL before being permanently mounted.

Masson Trichrome staining protocol

This staining procedure serves to stain collagen and mucus blue, while muscle, cytoplasm and neuroglia fibres should stain red with nuclei staining blue-black.

Paraffin sections were dewaxed in xylene and rehydrated through a series of alcohols to water using a Leica Autostainer XL ST5010 before incubation in Bouin's solution (Sigma HT10132) overnight at room temperature. The sections were then rinsed in running water with a final rinse in reverse osmosis (RO) water.

Sections were stained using a Masson Trichrome kit with Aniline Blue counterstain (Atom Scientific RRSK2) following the protocol included. First the nuclei were stained by immersing in Weigert's Iron Hematoxylin for 20 minutes (prepared immediately before use by mixing equal volumes of solution A and B) followed by a quick wash in water, differentiation in 0.5% acid alcohol solution and rinsing in running water. Sections were then stained with Ponceau Fuchsin solution for five minutes and following a quick rinse in water, differentiated and fixed in phosphotungstic acid for five minutes. Sections were transferred directly into Aniline blue Masson solution for five minutes then rinsed in RO water before further treatment in Phosphotungstic acid for five minutes. Sections were then transferred to acetic acid solution for five minutes and following a final rinse in RO water were dehydrated quickly in 99% industrial denatured alcohol (IDA), cleared in xylene and mounted.

BrdU labelling protocol

Paraffin sections were dewaxed in xylene and taken to alcohol using a Leica Autostainer XL ST5010. Any endogenous peroxidase activity was then blocked by immersing the sections in 1% H₂O₂ in methanol for 30 minutes. After washing in PBS, sections were treated in hot acid (1N HCl at 60°C) for eight minutes and then neutralized in boric acid buffer for six minutes. Following washing in PBS, the sections were blocked with 5% normal rabbit serum for 30 minutes before incubation with a rat IgG2a monoclonal anti BrdU antibody (AbD Serotec OBT0030S clone BU1/75(ICR1)) at a one in five dilution for one hour at room temperature. A negative primary control section was included to control for secondary reagent non specific staining. Sections were then washed in PBS before incubation with a secondary peroxidase conjugated rabbit anti-rat IgG antibody (Dako P0450) at one in one hundred diluted in 5% normal mouse serum for one hour. After further washing in PBS, labelling was visualised using 3,3'-Diaminobenzidine (DAB) peroxidase substrate (Vector ImmPACT SK-4105) for five minutes. Sections were then counterstained with hematoxylin, dehydrated and cleared in xylene using the Leica Autostainer XL before being permanently mounted.

RESULTS

Radiation-induced loss of body weight

The first symptom of radiation sickness in a mouse is weight loss. In laboratory studies of GI-ARS mice, weight loss increases due to dehydration during the diarrheal stage, when it may become necessary to humanely terminate a study. The extent of acute weight loss is radiation dose-dependent, but if the bone marrow is shielded many animals recover weight in the second week post irradiation, also in a broadly dose-dependent manner (Fig. 1). At doses less than 13 Gy (below the 20 day LD₃₀ for GI-ARS with PBI BM40) animals recovered their starting weight, although still not regaining weight to sufficiently match the unirradiated age-matched controls. At 13 Gy and higher (doses inducing GI-ARS) animals regained weight after the acute phase but then failed to gain weight over the following weeks. These animals displayed no other symptoms indicative of the prior irradiation other than that they gained weight more slowly than age matched unirradiated control mice. However, there then became a point at which some of the irradiated animals began to decline. This occurred in sporadic mice from two months post irradiation, with increasing dose-related frequency over the following months. Mice receiving less than 12 Gy remained unaffected. Control mice that received ciprofloxacin antibiotic support between days four and twenty did not gain weight at the same rate as the unsupported controls, but fewer mice became sick as a result of the DEARE following 13 Gy and 14 Gy than the unsupported mice receiving the same radiation dose. Above 14 Gy both groups of mice failed to consistently gain weight over the time course of the experiment.

Despite being inbred, similarly housed and irradiated at the same time of day, the long term response to the irradiation was quite variable within a dose treatment. The weight changes in a group of mice receiving 14 Gy and surviving GI-ARS are illustrated in Figure 2.

Examination of H & E cross sections of the small and large intestine from unirradiated mice reveal no histopathological differences between mice maintained on ciprofloxacin and those maintained unsupported other than acidified drinking water. Similarly, there were no notable differences post-irradiation in animals that succumbed to this delayed weight loss, whether on ciprofloxacin or not. The ciprofloxacin simply seemed to delay the development of the same histopathology (more subtle changes in barrier function, however, cannot be excluded).

The main early feature of mice aged after irradiation was the appearance in the small intestine and colon of circular cyst like structures, which look like early microadenomas (very similar structures to those seen in APC (adenomatous polyposis coli) mutant mice [analogous to human FAP (familial adenomatous polyposis coli), which predisposes people to intestinal tumors]. (Oshima et al. 1995, 1997; Potten et al. 2003). The cyst-like structures appeared within both the small and large intestines relatively soon after radiation exposure; examples are shown in Figure 3. These have been observed in samples as early as twenty days after radiation exposure. The incidence however, increased with both time and radiation dose (although a daily assessment for the full timecourse to plot the changing incidence over time has not been performed). In the small intestine they were mainly in the jejunal region, whereas in the colon they were predominantly distal.

Radiation effect in intestinal crypts

Curiously, even within a similar region of intestine, the crypt sizes were quite variable (unlike control mice in which crypt sizes are very similar). Thus, within the ileum there were hyperplastic crypts which were either longer or wider (or both) than normal crypts. In other areas the crypts were shorter and thinner, although the shortening appeared to increase with time post irradiation. Often both morphologies were seen within close proximity to each

other. The sizes of the villi were also variable. In some regions there were longer villi, in other areas the villi appeared shorter and wider. A consistent feature at 14 Gy and higher were more crypts undergoing bifurcation than in the control mice. Coupled with this was the presence of several crypts containing lots of mitotic cells. In normal mucosa levels of apoptosis are low, but this was also elevated. Examples are shown in Figure 4. This was consistent with crypt hyperplasia, bifurcation and possible adenoma formation, but inconsistent with shorter crypts and villus blunting. Crypt cell turnover was therefore variable and possibly deregulated.

Given that H & E stained slides showed that some intestines exhibited a shortening of the crypts and villi, the levels of proliferation were assessed via BrdU incorporation. BrdU was injected into the animals forty minutes before euthanasia, so labeled cells are indicative of the number of cells in the S phase of the cell cycle immediately prior to euthanasia. It was seen, especially in the lower ileum, that levels of BrdU labeling were much lower than in the age matched controls (Fig. 5). It was also noted that these sections contained smaller crypts and villi, confirming reduced cell production. The diameter of the intestine as a whole was also much smaller in these mice.

Intestinal tissue effects: muscularis mucosa, cellularity, collagen formation

There was a thickening of the muscle in many of the irradiated samples compared to control (also seen in Fig. 5). In the most severe cases the effects were clearly obvious, whereas in the moderate cases only certain areas of the intestine appear affected. However, it is difficult to conclusively exclude the effect of a tissue sectioning artifact due to orientation of the tissue during sectioning on this observation. The submucosa, however, was consistently expanded with a reduced mesenchymal cell density. Evidence of vascular structures with irregular shapes and expanded diameters was also seen. Similarly the cellularity of the upper villus was reduced, although there were frequently highly packed cells around the crypt villus junction.

Sections were also stained with Masson Trichrome, a histological stain for collagen and hence an indicator of fibrosis. In the age matched unirradiated mice a narrow, darkly stained band of collagen (blue) is seen in the submucosa. In a few of the older, unirradiated mice the band was wider and slightly paler, with increased staining within the villus lamina propria. Although it has not been quantified in the irradiated samples, however, the collagen band width appeared to increase far earlier (at an earlier age) and by a greater degree in many of the mice (Fig. 6, 7). There was also more collagen staining in the villus lamina propria. Overall there was a much greater total area of staining in the older irradiated mice. This staining was often less intense than in the age matched controls. The staining was also less organized, possibly indicative of collagen deposition and or remodeling. Future image analysis may enable quantification of the collagen levels within the crypt and villus submucosa.

Mice with signs of DEARE exhibited all the above morphologies in the same area of the intestine, i.e. areas with smaller crypts showed less BrdU labeling and a broader and paler band of collagen staining. However, there was a variation in the number and size of these foci between mice.

DISCUSSION

The dose response studies indicated that the delayed effects were only prevalent at radiation doses that also induced GI-ARS, suggesting that the initial mucosal breakdown and repair is a pre-requisite for later pathologies. This is consistent with previous more generic suggestions that the probability of symptomatic late radiation toxicity is minimal if the

radiation dose is below the acute tolerance level (Perez et al 2004). Unlike man, or non human primates, there was no evidence of continued intermittent diarrhea in mice allowed to age after surviving GI-ARS. The only obvious difference between the species that may be related to this observation is that mice do not develop granulation tissue (Sartor 1997).

Other than the weight changes associated with GI-ARS and the slower overall weight gain the mice were completely symptomless until the onset of late stage weight loss. During this symptomless period however, the mice were developing microadenomatous structures, of very similar appearance to those found in mice with a mutation in the APC. This is consistent with increases in gastrointestinal cancer following radiation exposure (Ron et al 1994, Preston et al 2007), and attributed to errors induced during DNA repair and tissue regeneration.

The observation that treatment of control mice with ciprofloxacin support for sixteen days provoked a long term reduction in animal weight gain was surprising and does not appear to be reported elsewhere.

The onset of DEARE was clearly delayed by the presence of ciprofloxacin, suggesting that the consequences of a reduction in enteric flora from days four to twenty had a much longer term effect on the intestine. The physical damage to the epithelium (levels of clonogen death) is consistent with or without the antibiotic, suggesting that the inflammatory response induced by the presence of the bacteria is responsible for the changed DEARE. These observations support reports that in addition to its antibiotic function ciprofloxacin may alleviate excessive pro-inflammatory responses mediating local gut injury (Lahat et al. 2007). Changed levels of bacterial challenge post irradiation may also impact the severity of the local mast cell response in GI-ARS, with consequences for mast cell involvement in DEARE-related fibrosis.

There has been evidence that long term changes to the endothelial function are involved in the development of late effects (Wang et al 2002, 2007, Lyubimova and Hopewell 2004, Rezvani et al. 1995), although the suggestion that damage to the endothelium was responsible for GI-ARS has now been largely refuted (Hendry et al. 2001, Schuller et al. 2006). Longer term effects may be due to changed regulation of thrombin and thrombomodulin, causing induced vascular permeability and thrombin activated inflammation and fibroblast activation (Wang et al. 2007). Activated fibroblasts produce transforming growth factor-beta1 (TGFbeta1) which in turn activates connective tissue growth factor (CTGF). TGFbeta1-mediated activation of CTGF is controlled by Smads, but recently Rho/ROCK signalling has been proposed as an alternative pathway involved in intestinal fibrosis (Haydont et al. 2007, Gervaz et al. 2009). The latter opens the possibility of using statins or Fasudil as potential delayed effect treatments, since they inhibit Rho and ROCK respectively (Haydont et al. 2007). Since the Rho pathway is also involved in vascular permeability, this may also have earlier stage therapeutic potential.

One of the consequences of fibroblast, myofibroblast and smooth muscle cell activation is the secretion of the fibrillar collagens (type I and III) (Matthes et al. 1992, Graham 1995). Thus, TGFbeta1 or Rho:ROCK pathways induce collagen production. It can also be induced by direct autocrine induction of CTGF (Yarnold and Brotons 2010). The increased collagen deposition in this study is consistent with this and many previous observations. Increased type I collagen, matrix metalloproteinases (MMPs) and their tissue inhibitors (TIMPs) have been described in the late phases of radiation enteritis and fibrosis (Remy et al. 1991, Strup-Perrot et al. 2004). Classically, radiation fibrosis was considered a chronic, progressive disease. However, more recently fibrosis has been defined as a dynamic process involving cycles of tissue remodeling by the MMPs and TIMPs. Cycles of collagen production and

tissue remodeling will undoubtedly also alter the composition of both the epithelial crypt clonogenic cell extracellular matrix niche and the growth factors it sequesters. Thus, there is both a direct and indirect effect of high dose radiation on the epithelium; the direct GI-ARS effect induced by clonogen (and hence crypt) death and the longer term indirect effect of local growth factor control of clonogen function. Assuming that there are cycles or 'flare ups' of inflammation during the development of DEARE, with concomitant cycles of stimulation and inhibition of crypt cell proliferation, this may account for some of the variability seen in cross sections from various mice. The Rho pathway is also implied in tumor hyperplasia (Gaugler et al. 2005) and so may well be involved in the regional variations in crypt proliferation and development of the microadenomas observed in this study.

A feature of these studies was the changed crypt cell proliferation in the mice. This was not consistently increased or decreased, but quite variable, particularly following the lower radiation doses or shorter times post-irradiation. In the early stages of DEARE (late GI-ARS) it may be expected to see a sustained reparative increase in crypt cell proliferation, with overshoots in cell production being subject to homeostatic feedback and gradually damping down of the system as the tissue is repaired and steady state levels resume. Increased cell production and crypt length has also been shown to cause increased crypt fission, which will ultimately restore crypt numbers. These processes are associated with a restoration of the clonogenic cell population by symmetrical expansion of the surviving clonogens. Replication and perpetuation of the template strand DNA, which may be damaged by the radiation exposure, can therefore contribute to increased early initiation of microadenomas (normally associated with aging).

As the DEARE symptoms progressed however, there was a consistently observed reduction in crypt cell proliferation. This may be real or be the result of reduced appetite in increasingly sick mice (fasting has been shown to reduce intestinal cell proliferation). Whilst the observation was indeed greatest in the animals that had lost the most weight, this alone cannot explain the fewer crypts and larger villi that were also observed in the mice experiencing DEARE. Interestingly this histopathology was very similar to that seen in geriatric mice (Fig. 8). Geriatric mice have also been described as having large 'bloated' villi with a reduced cellularity within the lamina propria core, along with a reduced overall crypt and villus number (Martin et al 1998a). The reduced surface area provided by fewer, larger, villi will limit the nutrient absorptive capacity, whilst the fibrotic core reduces the flexibility of these luminal protrusions and may impede the transit of the luminal contents. Together these may contribute to the malnutrition and constipation or other obstructive syndromes that occur in the elderly. If the same histopathology is also present at late times post irradiation in non human primates and man it may explain the similar problems of wasting, constipation and episodes of faecal urgency that are evident during DEARE.

A network model of aging has been proposed, called MARS (Kowald and Kirkwood 1996). This suggests that the processes that cause the aged phenotype are the accumulation of defective mitochondria leading to a reduced functional number; the accumulation of aberrant proteins; the effects of oxygen free radicals and reduced proteolytic scavengers. These are all processes that are also affected by irradiation, supporting parallels between the two responses.

The cells responsible for these long-term histopathology changes (be it aging or as a result of DEARE) must be long term residents of a tissue. The mesenchymal fibroblasts responsible for the collagen production undergo extended although ultimately finite replication and may therefore be responsible for the long term fibrotic changes. The crypt clonogenic epithelial cells are the long term cells responsible for the maintenance of the

mucosa. Under normal circumstances mice will undergo predominantly asymmetric division of their stem cells, generating daughter cells whilst maintaining their own population. Over years of daily division, with occasional exposures to genotoxic stresses and symmetrical divisions, there may be a gradual decline in stem cell fidelity and homeostatic regulation as they accumulate damage. In a post irradiation situation the surviving clonogens will be triggered to cycle rapidly in order to restore their number via symmetrical expansion. These cells will then restore the crypt structure, and then generate further crypts via crypt fission, each also developing a new stem cell hierarchy. Thus, sustained stem cell expansion is required in order to restore the tissue, followed by normal daily tissue maintenance. This process may therefore be equated to an accelerated aging process, compressing the events of several years into months.

Interestingly, geriatric mice displayed an altered response to injury in the small intestinal crypts, with delayed induction of p53 and p21 and changed apoptotic sensitivity in the clonogenic stem cells (Martin et al. 2000). The aged crypts were also slower to respond following high dose irradiation than younger adults, although the total number of cells with clonogenic potential was estimated to be higher (Martin et al. 1998b). This suggested that cells higher up the normal lineage may be recruited into the clonogenic compartment, possibly indicative of a deterioration of the crypt organisation. These more mature clonogens may be responsible for the reduced efficiency of the damage response.

Similarly impaired clonogen functional integrity in intestinal crypts from animals experiencing DEARE is also highly likely given that the nascent crypts generated post GI-ARS may be generated from recruited clonogens. Unfortunately, unlike the bone marrow, it is not possible to perform serial transplants in order to compare the long term functionality of the clonogens isolated from the different animals (adult, geriatric and those experiencing DEARE). It will, however, be interesting to determine their responses using the dose response and split radiation dose assays of Potten and Hendry (1985; Hendry et al. 1992; Roberts et al 1995) and also determine whether the extensive mucosal repair following GI-ARS has resulted in the generation of many 'poor quality' clonogens or simply accelerated clonal exhaustion.

CONCLUSION

It is clear that there are pathological changes in the intestine associated with DEARE. The GI-DEARE syndrome was seen at doses greater than 12 Gy, with a dose-related increase in observed pathologies. After 20 days mice developed structures similar to early adenomas. By day 75 most mice had such structures in both the small and large intestine, and many gradually became moribund. Abnormally high levels of apoptotic and mitotic cells were present in some crypts, along with early adenomas, suggesting tissue regeneration and areas of deregulated cell turnover. Over time the many crypts and villi also became blunted. A larger and fibrotic submucosa developed. Together these may lead to a reduced functional surface area and less motile intestine. These observations are similar to those seen in geriatric animals, suggesting that radiation exposures that cause DEARE may induce a premature aging of the GI tract.

Acknowledgments

This work supported by NIAID contracts HHSN266200500043C and HHSN272201000046C.

REFERENCES

Andreyev J. Gastrointestinal complications of pelvic radiotherapy: Are they of importance. *Gut*. 2005; 54:1051–1054. [PubMed: 16009675]

- Boggs DR. The total marrow mass of the mouse: a simplified method of measurement. *Am J Hematol*. 1984; 16(3):277–286. [PubMed: 6711557]
- Coia LR, Myerson RJ, Tepper JE. Late effects of radiation therapy on the gastrointestinal tract. *Intl J Radiat Oncol Biol Phys*. 1995; 31(5):1213–1236.
- Dubios A, Walker RI. Prospects for management of gastrointestinal injury associated with the acute radiation syndrome. *Gastroenterology*. 1988; 95:500–507. [PubMed: 3292340]
- Gaugler MH, Vereycken-Holler V, Squiban C, Vandamme M, Vozenin-Brotons MC, Benderitter M. Pravastatin limits endothelial activation after irradiation and decreases the resulting inflammatory and thrombotic responses. *Radiat Res*. 2005; 163(5):479–487. [PubMed: 15850408]
- Gervaz P, Morel P, Vozenin-Brotons MC. Molecular aspects of intestinal radiation-induced fibrosis. *Curr Mol Med*. 2009; 9(3):273–280. [PubMed: 19355909]
- Goodman MT, Mabuchi K, Morita M, Soda M, Ochikubo S, Fukuhara T, Ikeda T, Terasaki M. Cancer incidence in Hiroshima and Nagasaki, Japan, 1958–1987. *Eur J Cancer*. 1994; 30A(6):801–807. [PubMed: 7917541]
- Graham MF. Pathogenesis of intestinal strictures in Crohn's disease—An update. *Inflamm Bowel Dis*. 1995; 1(3):220–227. [PubMed: 23282393]
- Hauer-Jensen M. Late radiation injury of the small intestine. Clinical, pathophysiologic and radiobiologic aspects. A review. *Acta Oncol*. 1990; 29(4):401–415. [PubMed: 2202341]
- Hauer-Jensen M, Wang J, Denham JW. Bowel injury: Current and evolving management strategies. *Seminars in Radiation Oncology*. 2003; 13 357-271.
- Haydont V, Bourgier C, Vozenin-Brontons MC. Rho/ROCK pathway as a molecular target for modulation of intestinal-induced toxicity. *Brit J Radiol*. 2007; 80:S32–S40. [PubMed: 17704324]
- Hendry JH, Roberts SA, Potten CS. The clonogen content of murine intestinal crypts: Dependence on radiation dose used in its determination. *Radiat Res*. 1992; 132(1):115–119. [PubMed: 1410267]
- Hendry JH, Potten CS, Booth C. Endothelial cells and radiation gastrointestinal syndrome: Technical Comments. *Science*. 2001; 294(5546):1411. [PubMed: 11826850]
- Johnson RJ, Carrington BM. Pelvic radiation disease. *Clin. Radiol*. 1992; 45:4–12. [PubMed: 1740035]
- Kao MS. Intestinal complications of radiotherapy in gynecological malignancy – clinical presentation and management. *Intl. J. Gynecol. Obstet*. 1995; 49(suppl):S69–S75.
- Kowald A, Kirkwood TB. A network theory of ageing: the interactions of defective mitochondria, aberrant proteins, free radicals and scavengers in the ageing process. *Mutat Res*. 1996; 316(5–6): 209–236. [PubMed: 8649456]
- Lahat G, Halperin D, Barazovsky E, Shalit I, Rabau M, Klausner J, Fabian I. Immunomodulatory effects of ciprofloxacin in TNBS-induced colitis in mice. *Inflamm Bowel Dis*. 2007; 13(5):557–565. [PubMed: 17253612]
- Langberg CW, Sauer T, Reitan JB, Hauer-Jensen M. Relationship between intestinal fibrosis and histopathologic and morphometric changes in consequential and late radiation enteropathy. *Acta Oncol*. 1996; 35(1):81–87. [PubMed: 8619945]
- Lyubimova N, Hopewell JW. Experimental evidence to support the hypothesis that damage to the vascular epithelium plays the primary role in the development of late radiation induced CNS injury. *Br J Radiol*. 2004; 77(918):488–492. [PubMed: 15151969]
- Martin K, Kirkwood TB, Potten CS. Age changes in stem cells of murine small intestinal crypts. *Exp Cell Res*. 1998a; 241(2):316–323. [PubMed: 9637773]
- Martin K, Potten CS, Roberts SA, Kirkwood TB. Altered stem cell regeneration in irradiated intestinal crypts of senescent mice. *J Cell Sci*. 1998b; 111(pt16):2297–2303. [PubMed: 9683625]
- Martin K, Potten CS, Roberts SA, Kirkwood TB. Age-related changes in irradiation induced apoptosis and expression of p21 and p53 in crypt stem cells of murine intestine. *Annals NY Acad Sci*. 2000; 908:315–318.
- Matthes H, Herbst H, Schuppan D, Stallmach A, Milani S, Stein H, Riecken EO. Cellular localization of procollagen gene transcripts in inflammatory bowel diseases. *Gastroenterology*. 1992; 102(2): 431–442. [PubMed: 1732114]

- Oshima H, Oshima M, Kobayashi M, Tsutsumi M, Taketo MM. Morphological and molecular processes of polyp formation in Apc(delta716) knockout mice. *Cancer Res.* 1997; 57(9):1644–1649. [PubMed: 9135000]
- Oshima M, Oshima H, Kitagawa K, Kobayashi M, Itakura C, Taketo M. Loss of Apc heterozygosity and abnormal tissue building in nascent intestinal polyps in mice carrying a truncated Apc gene. *Proc Natl Acad Sci U S A.* 1995; 92(10):4482–4486. [PubMed: 7753829]
- Perez, CA.; Brady, LW.; Halperin, EC.; Schmidt-Ullrich, RK. Principles and practice of radiation oncology. 4th Ed. Philadelphia Pa: Lippincott, Williams and Wilkins; 2004.
- Potten, CS.; Hendry, JH. The microcolony assay in mouse small intestine. In: Potten, CS.; Hendry, JH., editors. *Cell Clones: Manual of Mammalian Cell Techniques.* Livingstone, Edinburgh: Churchill; 1985. p. 50-60.
- Potten CS, Booth C, Tudor GL, Booth D, Brady G, Hurley P, Ashton G, Clarke R, Sakakibara S, Okano H. Identification of a putative intestinal stem cell and early lineage marker; musashi-1. *Differentiation.* 2003; 71(1):28–41. [PubMed: 12558601]
- Preston DL, Ron E, Tokuoka S, Funamoto S, Nishi N, Soda M, Mabuchi K, Kodama K. Solid cancer incidence in atomic bomb survivors: 1958–1998. *Radiat Res.* 2007; 168(1):1–64. [PubMed: 17722996]
- Remy J, Wegrowski J, Crechet F, Martin M, Daburon F. Long-term overproduction of collagen in radiation-induced fibrosis. *Radiat Res.* 1991; 125(1):14–19. [PubMed: 1986396]
- Rezvani M, Hopewell JW, Robbins ME. Initiation on non-neoplastic late effects: the role of the endothelium and connective tissue. *Stem Cells.* 1995; 13(Suppl 1):248–256. [PubMed: 7488953]
- Roberts SA, Hendry JH, Potten CS. Deduction of the clonogen content of intestinal crypts: a direct comparison of two-dose and multiple-dose methodologies. *Radiat Res.* 1995; 141(3):303–308. [PubMed: 7871157]
- Ron E, Preston DL, Mabuchi K, Thompson DE, Soda M. Cancer incidence in atomic bomb survivors. Part IV: Comparison of cancer incidence and mortality. *Radiat Res.* 1994; 137(Suppl 2):S98–S112. [PubMed: 8127954]
- Sartor RB. Pathogenesis and immune mechanisms of chronic inflammatory bowel diseases. *Am J Gastroenterol.* 1997; 92(12 Suppl):5S–11S. [PubMed: 9395346]
- Schuller BW, Binns PJ, Riley KJ, Ma L, Hawthorne MF, Coderre JA. Selective irradiation of the vascular endothelium has no effect on the survival of murine intestinal crypt stem cells. *Proc Natl Acad Sci USA.* 2006; 103(10):3787–3792. [PubMed: 16505359]
- Strup-Perrot C, Mathé D, Linard C, Violot D, Milliat F, François A, Bourhis J, Vozenin-Brotans MC. Global gene expression profiles reveal an increase in mRNA levels of collagens, MMPs, and TIMPs in late radiation enteritis. *Am J Physiol Gastrointest Liver Physiol.* 2004; 287(4):G875–G885. [PubMed: 15178550]
- Thompson DE, Mabuchi K, Ron E, Soda M, Tokunaga M, Ochikubo S, Sugimoto S, Ikeda T, Terasaki M, Izumi S. Cancer incidence in atomic bomb survivors. Part II: Solid tumors, 1958–1987. *Radiat Res.* 1994; 137(2 Suppl):S17–S67. [PubMed: 8127952]
- Wang J, Boerma M, Fu Q, Hauer-Jensen M. Significance of endothelial dysfunction in the pathogenesis of early and delayed radiation enteropathy. *World J Gastroenterol.* 2007; 13(22):3047–3055. [PubMed: 17589919]
- Wang J, Zheng H, Ou X, Fink LM, Hauer-Jensen M. Deficiency of microvascular thrombomodulin and up-regulation of protease activated receptor-1 in irradiated rat intestine: possible link between endothelial dysfunction and chronic radiation fibrosis. *Am J Pathol.* 2002; 160(6):2063–2072. [PubMed: 12057911]
- Yarnold J, Brotans MC. Pathogenetic mechanisms in radiation fibrosis. *Radiother Oncol.* 2010; 97(1):149–161. [PubMed: 20888056]

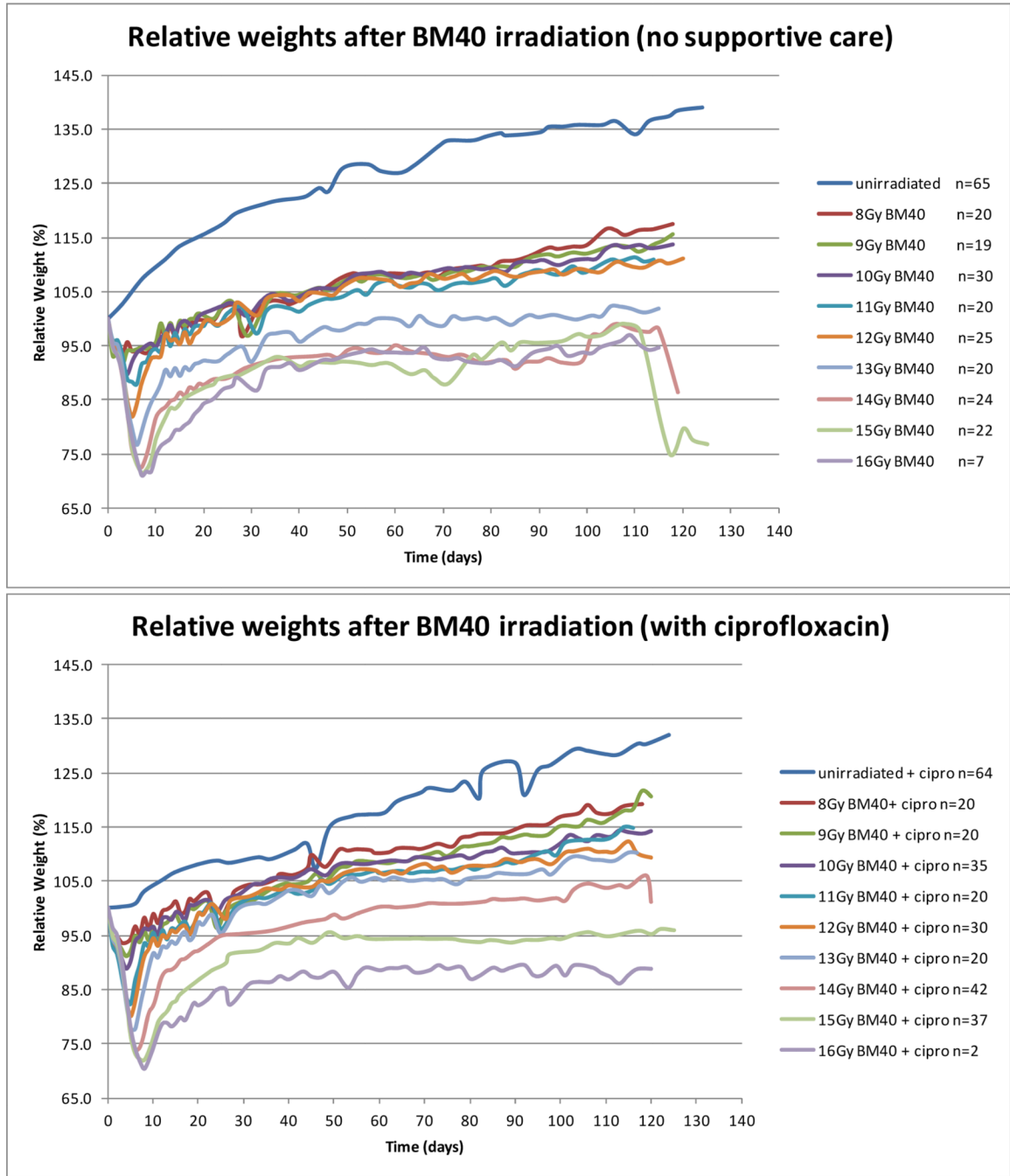


Figure 1. Weight loss changes post irradiation. The number of animals shown is the number surviving after day 20 from all DEARE studies. Animals were euthanized as scheduled on day 75 or 120, or due to sickness. Animals were euthanized when weight loss exceeded 20% and the animals also exhibited moribund symptoms. Weight gain was reduced in control mice by the presence of ciprofloxacin. After an initial radiation dose dependent weight loss, animals regained weight. All radiation exposures impeded the subsequent weight gain, with the greatest impact at 13 Gy and higher. Antibiotic supportive care may be beneficial at these higher doses.

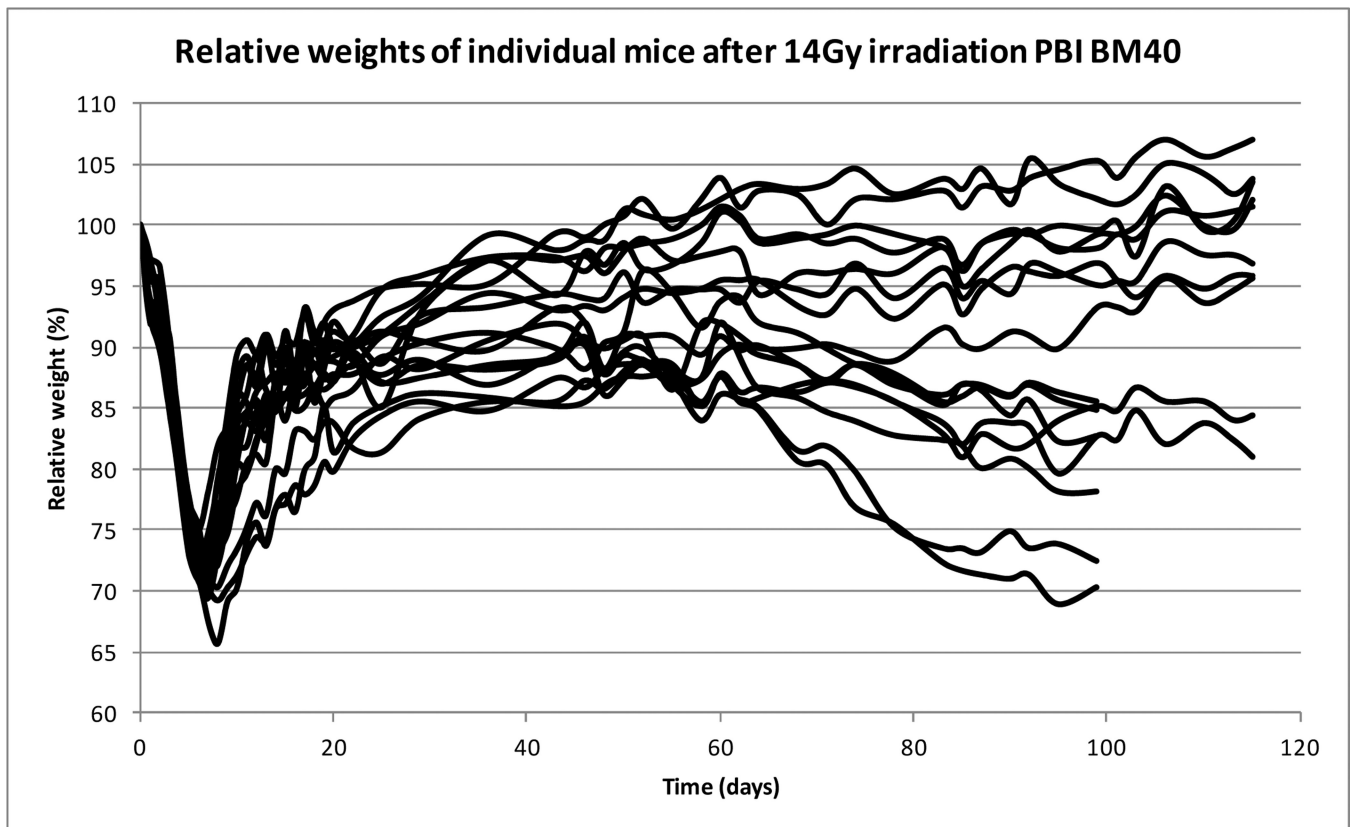


Figure 2. Weight loss changes post irradiation. An example of the variation within the same treatment group. Some animals appeared healthy and gained weight, whereas others lost weight and in extreme cases became moribund.

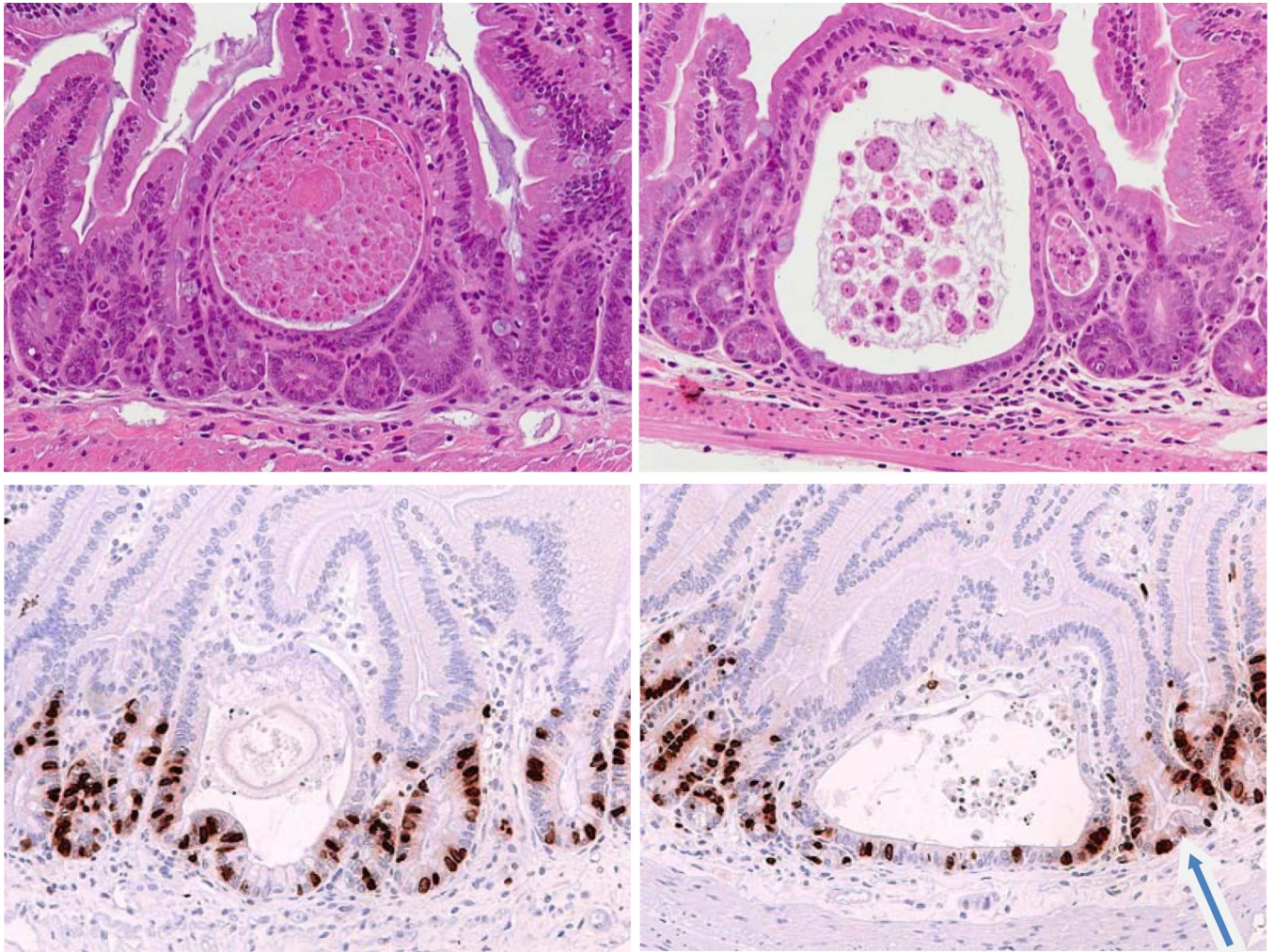


Figure 3. Examples of lesions similar to microadenomas in animals exposed to irradiation (typical of lesions seen from 20–200 days post irradiation at doses above 12Gy irrespective of ciprofloxacin treatment). Top: H & E sections of small intestine show examples of the abnormal pathologies seen in DEARE mice four months following 14Gy. The cyst-like structures are typical of microadenomas. Bottom: Similar structures from mice four months following 16Gy, labeled to reveal BrdU labelled cycling cells. The arrow indicates a bifurcating crypt adjacent to a microadenoma.

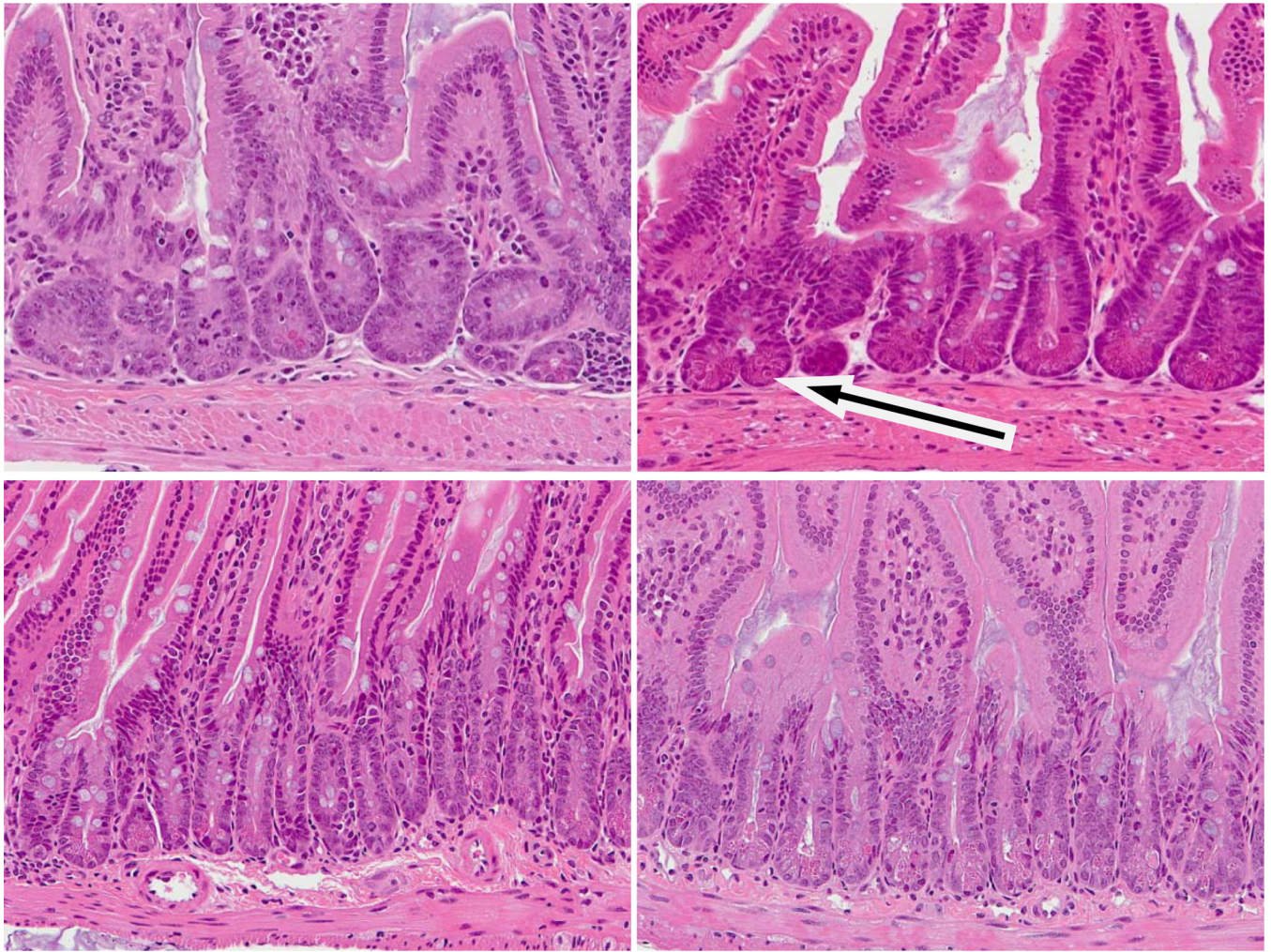


Figure 4.

Examples of changed crypt cell turnover in DEARE mice at a range of doses. Top: Animals four months post irradiation. Bottom: Age matched controls. Post irradiation crypts and villi were both smaller than the controls. Several crypts contained multiple mitotic cells and high levels of crypt fission were seen (arrow). Increased levels of apoptosis (as judged by the stereotypical condensed chromatin and eosinophilic staining) were often observed, often at high cell positions.

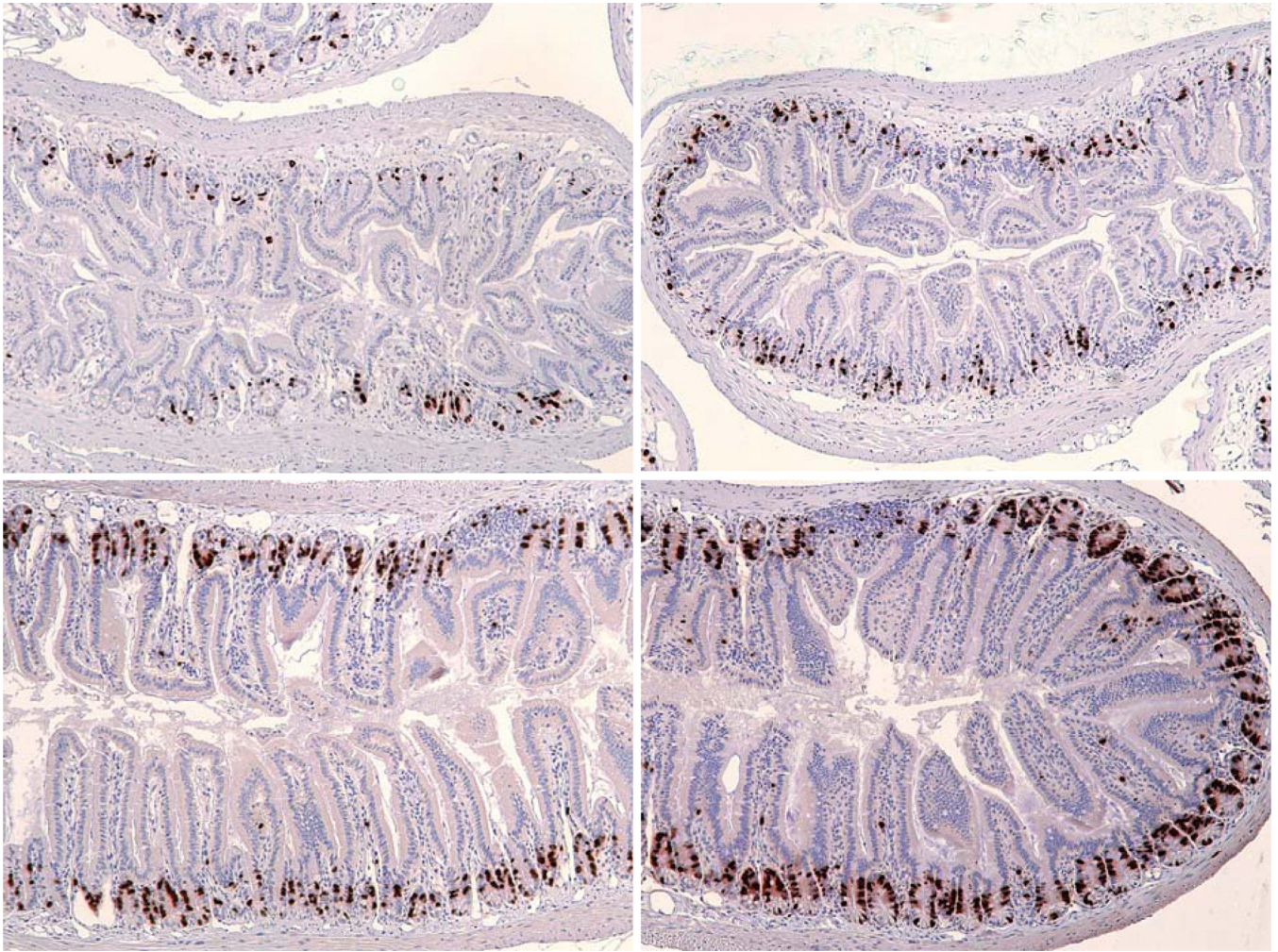


Figure 5. BrdU labeling in moribund DEARE mice. Mice were injected with BrdU 40 minutes prior to euthanasia and the incorporation revealed by immunohistochemistry. Top: Day 94 following 14 Gy (left), Day 192 following 15 Gy (right). Note the thicker submucosa and the shorter crypts and villi. The diameter of the intestine as a whole is also smaller. Bottom: Unirradiated controls, day 125 (left), day 200 (right).

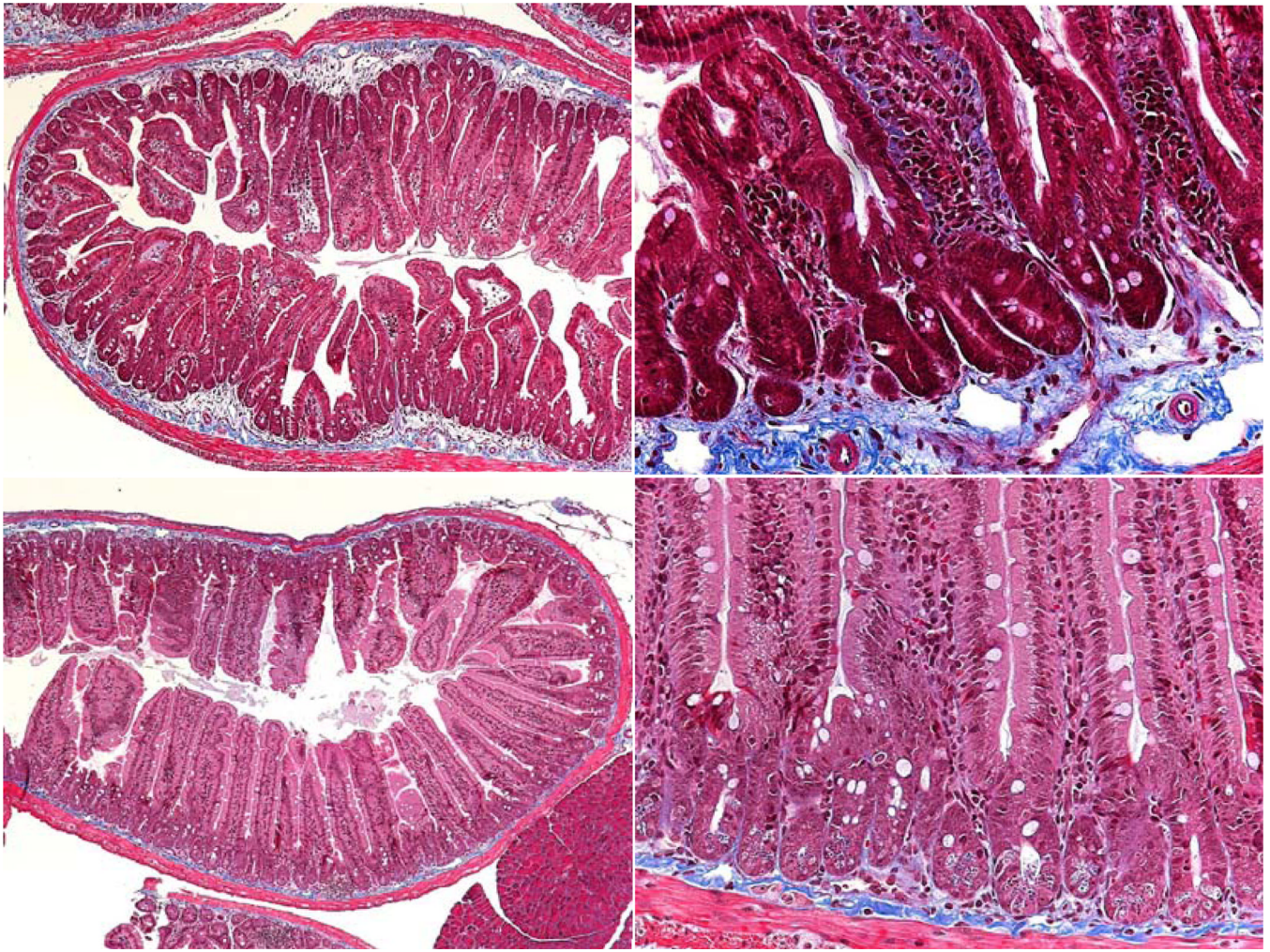


Figure 6. Masson Trichrome staining in moribund DEARE mice. Top: Day 112 following 16 Gy (left) and day 119 following 14 Gy (right). Bottom: Unirradiated controls, day 125. The increased collagen (blue stain) in the irradiated mice is clearly visible.

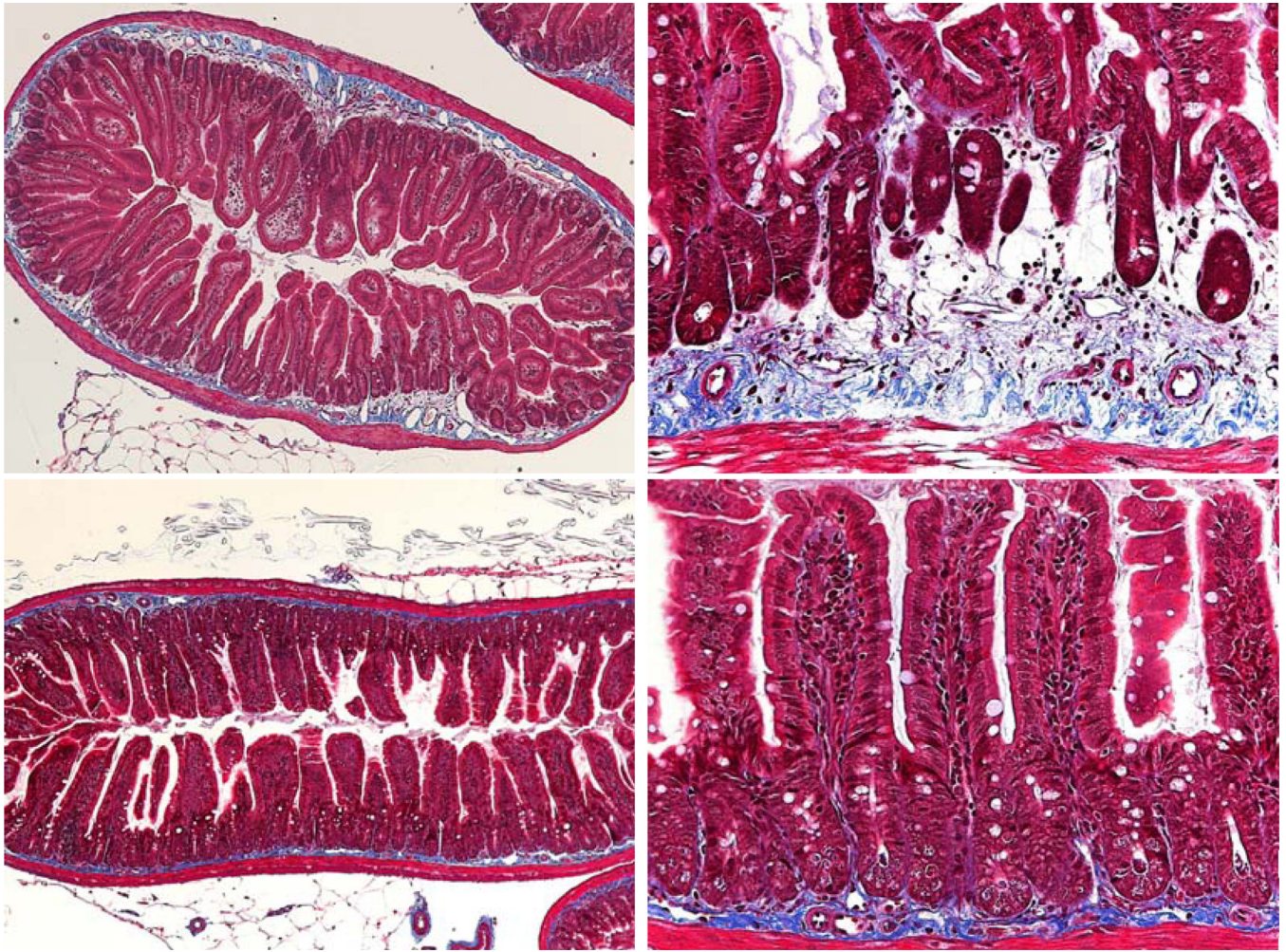


Figure 7. Masson Trichrome staining in older moribund DEARE mice. Top: Day 192 following 15 Gy. Bottom: Unirradiator controls, day 200.

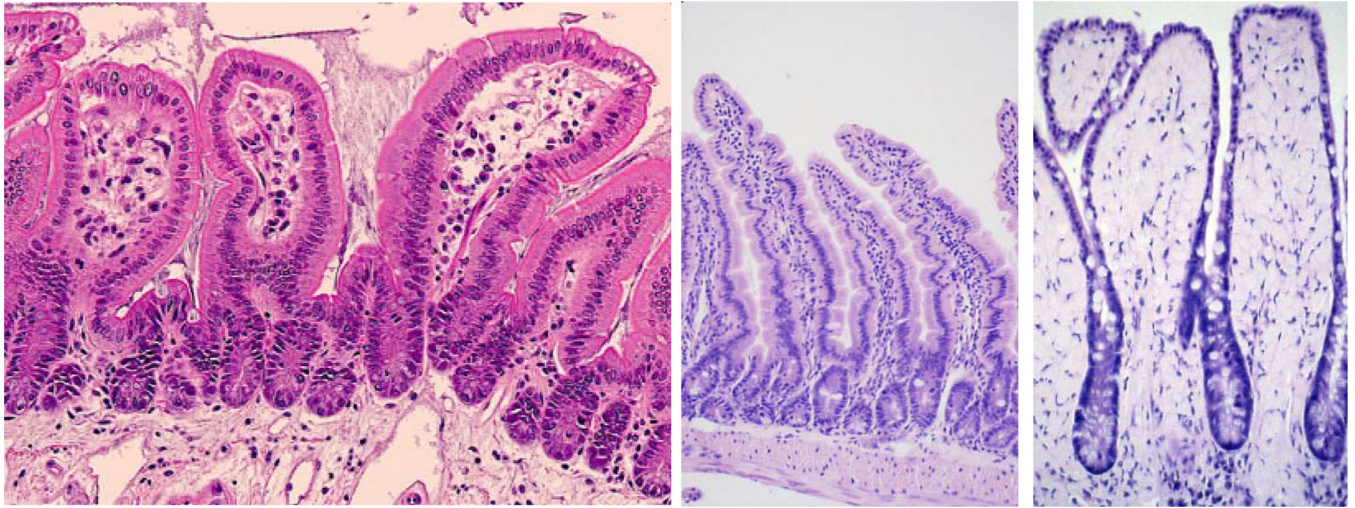


Figure 8.

Example of the similarity between aged and DEARE mice. Left: H & E section of a 15 Gy day 192 sample. The villi are short and wide with fewer cells in the lamina propria. Mid: A control 5 month old mouse with longer villi and normal looking lamina propria. Right: A 32 month old mouse. The broad spade-like villi result in a reduced absorptive surface area and a less flexible structure, both of which contribute to a failure to thrive.